Article

J. Biol. Regul. Homeost. Agents. 2024; 38(6): 4815–4823
https://doi.org/10.23812/j.biol.regul.homeost.agents.20243806.384

Increased FTO Expression Demethylates XBP1 m^{6}A, Thereby Regulating XBP1-C/EBPα and Promoting Hepatocellular Carcinoma Growth

Chen Xu[1], Liangjun Jiang[2], Xianzhou Lu[1,*], Wei Li[1,*]

[1]The Affiliated Nanhua Hospital, Department of Hepatobiliary Surgery, Hengyang Medical School, University of South China, 421002 Hengyang, Hunan, China
[2]The Affiliated Nanhua Hospital, Department of Gastroenterology, Hengyang Medical School, University of South China, 421002 Hengyang, Hunan, China
*Correspondence: lxz0734@126.com (Xianzhou Lu); Liweiping0734@126.com (Wei Li)
Submitted: 18 February 2024 Revised: 12 March 2024 Accepted: 15 March 2024 Published: 1 June 2024

Background: N6-methyladenosine (m^{6}A) modification predominantly occurs in cancer cells mRNA. The X-box binding protein 1 (XBP1) influences hepatocellular carcinoma (HCC) progression, but its m^{6}A regulatory mechanism remains unclear. Furthermore, the dysregulation of CCAAT/enhancer binding proteins alpha (C/EBPα) in liver cancer is influenced by fat mass and obesity-associated protein (FTO) and acts downstream of XBP1. Therefore, this study aims to investigate how FTO catalyzes XBP1 m^{6}A demethylation in HCC regulation.

Methods: Initially, HepG2 cells were used to construct FTO overexpression and knockdown cells. The cells were divided into the FTO overexpression group (oe-FTO), overexpression control group (oe-NC), FTO knocked-down group (sh-FTO), and control of FTO knocked-down group (sh-NC) groups. RNA immunoprecipitation quantitative polymerase chain reaction (RIP-qPCR) was used to determine the interaction between FTO and XBP1. Furthermore, quantitative real time polymerase chain reaction (qRT-PCR) and Western blotting (WB) analysis were utilized to assess the expression levels of XBP1 and C/EBPα. Additionally, subcutaneous transplanted tumor models were constructed and the tumor size, weight, and occurrence time were monitored. Moreover, Hematoxylin-Eosin (H&E) staining was employed to observe the pathological changes of tumors. m^{6}A immunoprecipitation (MeRIP)-qPCR was used to evaluate the XBP1 m^{6}A modification levels. qRT-PCR and WB analysis were used to determine the expression levels of XBP1 and C/EBPα.

Results: We observed that FTO specifically binds to *XBP1* mRNA in HCC cells, indicating a potential regulatory role at the RNA level. At the cellular level, compared to the sh-NC and oe-NC groups, the m^{6}A methylation level of XBP1 was significantly increased in the sh-FTO group, while it was decreased in the oe-FTO group ($p < 0.05$). Furthermore, the mRNA and protein expression levels of FTO, XBP1, and C/EBPα were altered following FTO manipulation. Functional assays demonstrated that FTO overexpression promoted cell proliferation and invasion while inhibiting apoptosis. Conversely, FTO knockdown resulted in decreased cell proliferation and invasion and increased apoptosis. In a mouse xenograft tumor model, we observed rapidly growing tumors in the oe-FTO group, whereas sh-FTO tumors exhibited slower growth. Histological analysis revealed distinct patterns of tumor growth and damage. Collectively, these findings suggest that FTO plays a crucial role in HCC progression through its effects on XBP1 and C/EBPα, providing insights into the potential therapeutic intervention of FTO in hepatocellular carcinoma.

Conclusion: FTO overexpression leads to m^{6}A demethylation of XBP1, thereby modulating the expression of XBP1-C/EBPα and suppressing cell apoptosis. This, in turn, facilitates the progression of hepatocellular carcinoma by promoting cell growth.

Keywords: FTO; XBP1; m^{6}A demethylation; XBP1-C/EBPα

Introduction

Hepatocellular carcinoma (HCC) ranks as the third leading cause of cancer-related fatalities [1], constituting the predominant form of liver cancer at 85–90% [2]. Owing to the absence of distinct early-stage symptoms, HCC is often diagnosed at advanced stages, contributing to low 5-year survival rates following surgical interventions [3]. Addressing this challenge needs more targeted clinical approaches, necessitating comprehensive research into the pathogenesis of HCC.

The development of HCC is closely linked to a multitude of molecular biological processes, encompassing apoptosis, methylation modification, and immune regulation [4]. Importantly, among these mechanisms, N6-methyladenosine (m^{6}A) modification of mRNA stands out as the predominant form of methylation, regulated by both m^{6}A methyltransferases and demethylases [5]. The dys-

Journal of
BIOLOGICAL REGULATORS
and Homeostatic Agents

regulation of m^{6}A modification has been associated with various diseases, including but not limited to obesity [6], heart failure, and cancer [7]. The m^{6}A demethylase, fat mass and obesity-associated protein (FTO) are implicated in diverse cancer types. For instance, in bladder cancer, FTO modulates the MALAT/miR-384/MAL2 axis, thereby promoting the onset and progression of cancer [8]. In colorectal cancer, FTO contributes to chemotherapy resistance in cancer patients by inhibiting cell growth through SIVA1 [9]. X-box binding protein 1 (XBP1) functions as a transcription factor downstream of inositol-requiring enzyme 1α (IRE1α), which is a transmembrane protein serine/threonine kinase in the ER stress signaling pathway [10]. Extensive research has highlighted the crucial involvement of XBP1 in the progression of HCC. Particularly, the unspliced form of XBP1 has been identified as a promoter of tumor growth, exerting its influence by enhancing cholesterol biosynthesis in the context of HCC [11]. AGR2 modulates endoplasmic reticulum homeostasis through the IRE1α-XBP1 cascade, thereby regulating both the progression of HCC and its resistance to sorafenib [12]. Research has indicated the dysregulation of CCAAT/enhancer binding protein alpha (C/EBPα) in solid tumors, including those affecting the liver, breast, and lung [13]. Its role in tumor progression lies in its mediation of downstream signaling pathway molecules. In HCC, C/EBPα interacted with PPARγ to regulate the expression of FOXC1, thereby affecting tumor growth. Furthermore, inhibitors of FTO have been found to reduce intracellular lipid production by downregulating the expression of C/EBPα in breast cancer, offering insights for innovative tumor treatment [14]. Nevertheless, there is limited elucidation into the regulatory role of FTO on C/EBPα in HCC, and whether it orchestrates the XBP1-C/EBPα pathway by the demethylation of XBP1 m^{6}A, thereby fostering the growth of HCC cells.

This study involved the establishment of HCC models with both FTO knockdown and overexpression to investigate the interaction between m^{6}A methylation modification and XBP1, examining its impact on downstream signaling molecules of XBP1. Additionally, the investigation delved into the mechanism through which FTO catalyzes the demethylation of XBP1 m^{6}A to regulate HCC.

Materials and Methods

Reagents and Samples

HepG2 cell line was purchased from the American Culture Collection Center ATCC (Item number: HB-8065, Manthus, VA, USA) along with mycoplasma infection analysis, STR validation. The DMEM medium (10566016) and fetal calf serum (10100147) were purchased from Gibco (Grand Island, CA, USA). The BALB/c mice, produced by Charles River Laboratories, Japan, were purchased from Vitong Lihua Laboratory Animal Technology Co., Ltd. (Beijing, China). Magna m^{6}A immunoprecipitation (MeRIP)™ m^{6}A kit was purchased from Merck Millipore (#17-10499, Billerica, MA, USA). The Trizol reagent was obtained from Invitrogen (10296010, Carlsbad, CA, USA) and SYBR Green Pro Taq HS premixed qPCR kit (AG11728) was purchased from Acoray Biotech Co., Ltd. (Changsha, China). Bovine serum albumin BSA-V (A8020), BCA protein concentration assay kit (PC0020), and PBS powder (P1010) were purchased from Solarbio (Beijing, China). PVDF membrane (0.45 μm, number: IPVH00005) was purchased from Millipore (Billerica, MA, USA). β-actin (AF0003, 1:1000) and HRP conjugated goat anti-rabbit IgG (H+L) (A0208, 1:3000) were purchased from Beyotime (Shanghai, China). Antibodies including FTO (ab124892, 1:1000), XBP1 (ab37152, 1:500), C/EBPα (ab140479, 1:500), and HRP conjugated goat anti-mouse IgG (H+L) (ab205719, 1:3000) were purchased from Abcam (Cambridge, UK). The Hematoxylin-Eosin (H&E) staining kit was purchased from Sangon Bioengineering Co., Ltd. (Item number: E607318, Shanghai, China).

Cell Culture and Treatment

HepG2 cells were incubated in DMEM complete medium under standard culture conditions at 37 °C in the presence of 5% CO_2. Subsequently, these cells were distributed into 6-well plates at a density of 1×10^6 cells per well. The stable FTO knockdown or overexpression cells were established through the transfection of the cells with a lentiviral vector. The lentivirus construct was obtained from Shandong Weizhen Biological Technology Co., Ltd. Furthermore, the cells were divided into four groups: the FTO overexpression group (oe-FTO), the overexpression control group (oe-NC), the FTO knocked-down group (sh-FTO), and the control of FTO knocked-down group (sh-NC).

Plate Clone

HepG2 cells were seeded into 6-well plates at a density of 800 cells per well and incubated at 37 °C in the presence of 5% CO_2 for 10–14 days. Following this, the cells were fixed using 4% paraformaldehyde, stained with crystal violet dye for 5 minutes, and rinsed with water until eliminating the background color. Subsequently, the cell colonies were observed and photographed. The colony counting was performed utilizing the Image J software (V1.8.0.112, LOCI, University of Wisconsin, Madison, WI, USA).

Transwell Assay

Initially, the Transwell inserts were pre-coated with the matrix gel (approximately 50 μL per well) and allowed to be set for 30 minutes. The cells from each experimental group were seeded into culture plates and incubated for 24–36 hours. Following trypsin digestion, the cells were collected, thoroughly washed, and resuspended in the cul-

Table 1. A list of primers used in Real-Time Quantitative PCR (RT-qPCR) analysis.

Name	Forward primer	Reverse primer
FTO	5′-ACCTCCAGCATTAGATTC-3′	5′-GAAACTACCGCATTTACC-3′
XBP1	5′-TGCTGAGTCCGCAGCAGGTGC-3′	5′-GCTTGGCTGATGACGTCCCCAC-3′
C/EBPα	5′-CGGACTTGGTGCGTCTAAGATG-3′	5′-GCATTGGAGCGGTGAGTTTG-3′
GAPDH	5′-CGACCACTTTGTCAAGCTCA-3′	5′-AGGGGTCTACATGGCAACTG-3′

FTO, fat mass and obesity-associated protein; *XBP1*, X-box binding protein 1; *C/EBPα*, CCAAT/enhancer binding proteins alpha; *GAPDH*, glyceraldehyde-3-phosphate dehydrogenase.

ture medium. After assessing their count, the cells were inoculated into the upper chamber of the Transwell inserts at a density of 2×10^4 cells per well (with 3 replicate wells for each group). Following 48 hours of incubation, the non-penetrated cells were carefully swabbed from the membrane. The cells were then washed with PBS, fixed in a methanol solution for 20 minutes followed by staining with 0.1% crystal violet dye. Finally, the staining pattern and cell morphology were observed using a light microscope at 100× magnification.

Apoptosis Assays

After treatment, trypsin (R001100, ThermoFisher, Shanghai, China) was employed for cell digestion. The resulting cells underwent centrifugation, followed by a PBS wash and eventual resuspension in binding buffer. The apoptosis rate was assessed in each experimental group employing the Annexin V-PI Apoptosis Detection Kit I (WLA001a, Wanleibio, Shenyang, China), following the guidelines provided by the manufacturer. Finally, the cells underwent flow cytometry analysis using a Beckman instrument (B23317, Brea, CA, USA).

MeRIP-qPCR

Genesky Biotechnology (Shanghai, China) provided support for MeRIP sequencing and subsequent data analysis. The m^6A immunoprecipitation (MeRIP) procedure was conducted employing the Magna MeRIP™ m^6A kit, in adherence to the manufacturer's guidelines. Initially, mRNA underwent DNase I digestion, followed by fragmentation to approximately 100 nt using RNA fragmentation reagents. The resulting fragments were treated with stop buffer, subjected to standard ethanol precipitation, and then collected. Furthermore, 12 µg of anti-m^6A antibody and 50 µL of magnetic beads were mixed in IP buffer followed by incubation at room temperature for 1 hour. Subsequently, 6 µg of fragmented mRNA was added to the antibody-bead mixture and incubated at 4 °C with rotation for a duration of 4 hours. Following washing, the immunoprecipitation mixture underwent digestion with a high concentration of proteinase K. In the next step, the RNA that bound to the antibody was extracted using the phenol-chloroform and ethanol precipitation method, followed by qPCR analysis. The relative enrichment, normalized to the input, was expressed as $\%Input = 1/10 \times 2^{Ct[IP]-Ct[input]}$.

Real-Time Quantitative PCR (RT-qPCR)

Total RNA was extracted from cells or tissues using Trizol reagent and subsequently reverse transcribed into cDNA. PCR amplification was conducted utilizing the SYBR Green Pro Taq HS premixed qPCR kit, following the reagent instructions. Moreover, RT-qPCR analysis was performed utilizing ABI QuantStudio 5 Real-Time PCR Systems. Furthermore, the relative expression levels of the target genes were assessed using the $2^{-\Delta\Delta Ct}$ method. The primers used in RT-qPCR are shown in Table 1. These primers were designed by Sangon Bioengineering Co., Ltd. (Shanghai, China).

Western Blotting (WB)

Total protein was extracted from cells or tissues and quantified using a BCA kit. The proteins were resolved through 8% SDS-PAGE and subsequently transferred onto a PVDF membrane. The membrane was then blocked with a 5% BSA solution for 1 hour followed by washing with PBS. After this, the membrane was incubated overnight at 4 °C with the respective antibodies against XBP1, C/EBPα, FTO, and glyceraldehyde-3-phosphate dehydrogenase (GAPDH). The following day, the membrane was exposed to the corresponding secondary antibody for 1 hour. Finally, the immunoblots were observed using the Bio-Rad system and the grayscale values of the protein bands were determined through ImageJ software (V1.8.0.112, NIH, Madison, WI, USA).

Construction of Transplanted Tumor Model

BALB/c mice (n = 120), aged 8 weeks and weighing 25–30 g, were obtained from Hunan Sleek da Co., Ltd. The mice were randomly divided into 4 groups, with 30 animals in each group. Meanwhile, the mice were transplanted with (0.2 mL, 1×10^6) FTO overexpression, knockdown, and control cells, constructed in this study, to establish transplanted tumor models. The mice were divided into the following four groups: the oe-FTO group, the oe-NC group, the sh-FTO group, and the sh-NC group. They were carefully monitored for tumor size, weight, and occurrence. The data were analyzed through repeated measures analysis of variance method. For mice, we used an intraperitoneal injection of pentobarbital sodium (50 mg/kg) for euthanasia. According to the Standards for Humane Euthanasia of Laboratory Animals, it is recommended to end the life of an

Journal of
BIOLOGICAL REGULATORS
and Homeostatic Agents

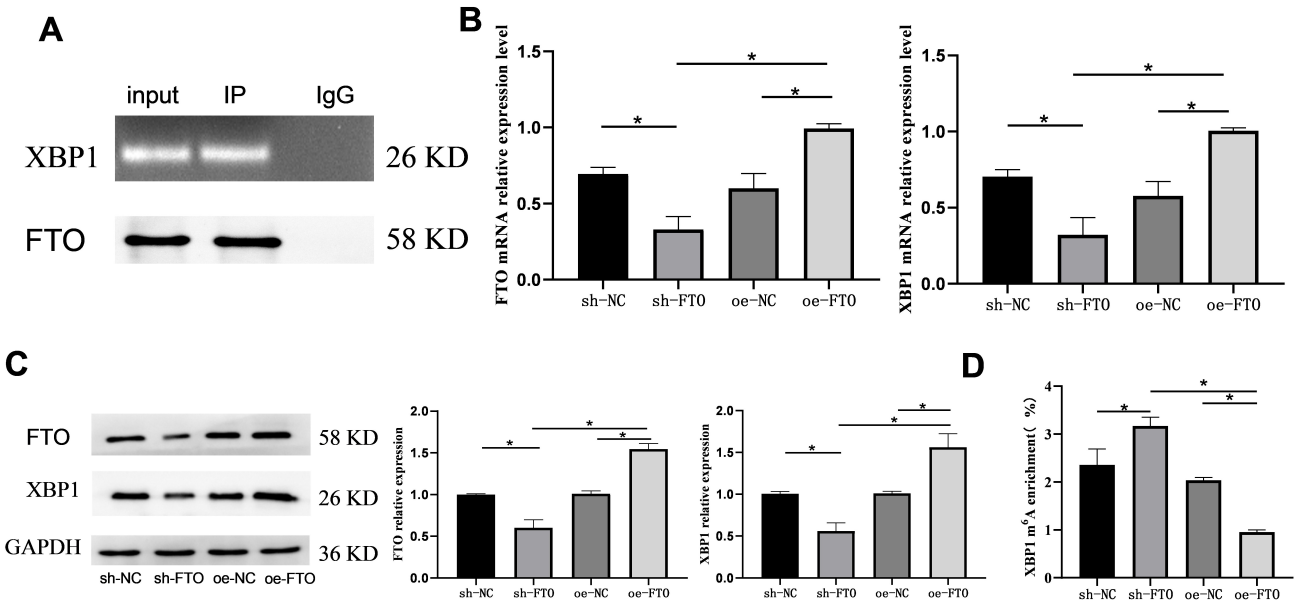

Fig. 1. Overexpression of FTO downregulated m^{6}A methylation of XBP1 in HCC cell. (A) Interaction between FTO and XBP 1 in cells was determined through m^{6}A immunoprecipitation (MeRIP)-qPCR. (B) The levels of *XBP 1* and *FTO* mRNA were determined using qPCR. (C) Western blotting (WB) analysis of XBP 1 and FTO protein expression. (D) MeRIP-qPCR was utilized to assess the effects of FTO overexpression and knockdown on XBP1 N6-methyladenosine (m^{6}A) methylation levels in each group of cells. *$p <$ 0.05. oe-FTO, FTO overexpression group; oe-NC, overexpression control group; sh-FTO, FTO knocked-down group; sh-NC, control of FTO knocked-down group.

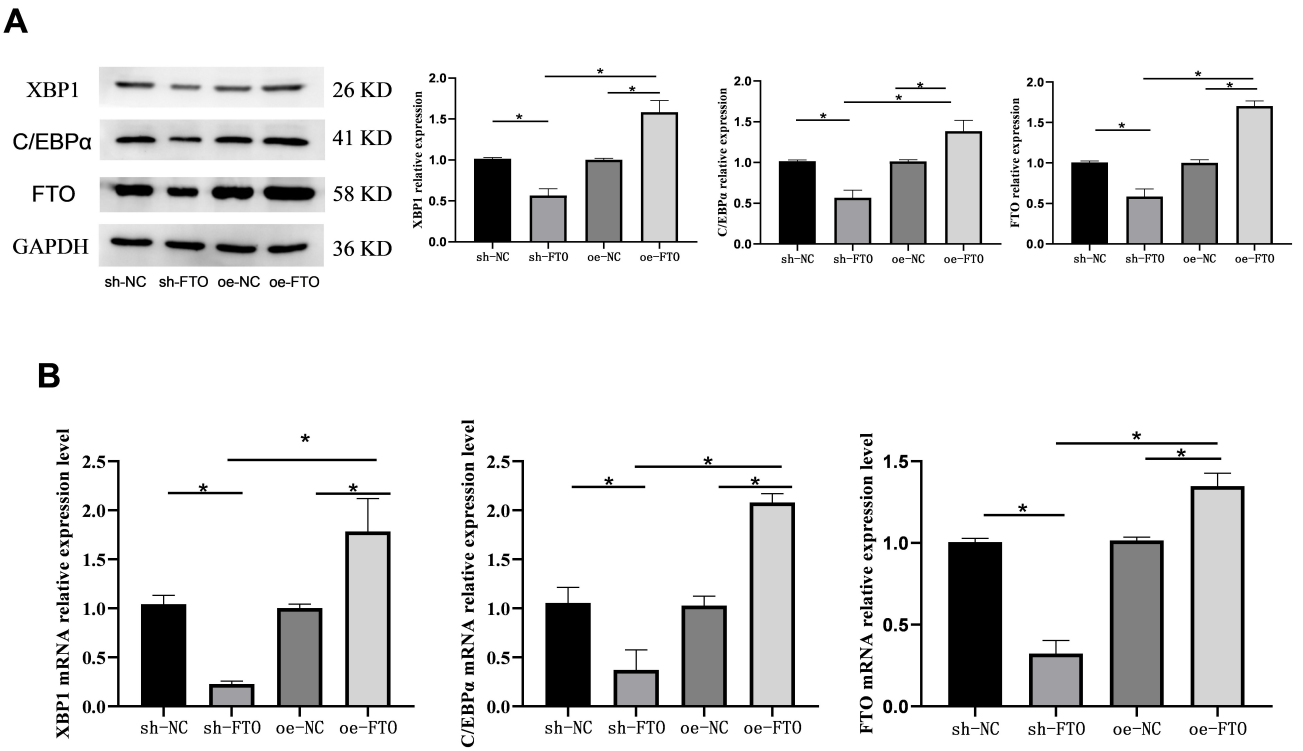

Fig. 2. Overexpression of FTO upregulated the expression of XBP1 and C/EBPα in HCC cells. (A) The expression levels of XBP1, C/EBPα, and FTO proteins were determined using WB analysis. (B) The levels of *XBP1*, *C/EBPα*, and *FTO* mRNA were determined using PCR. *$p < 0.05$.

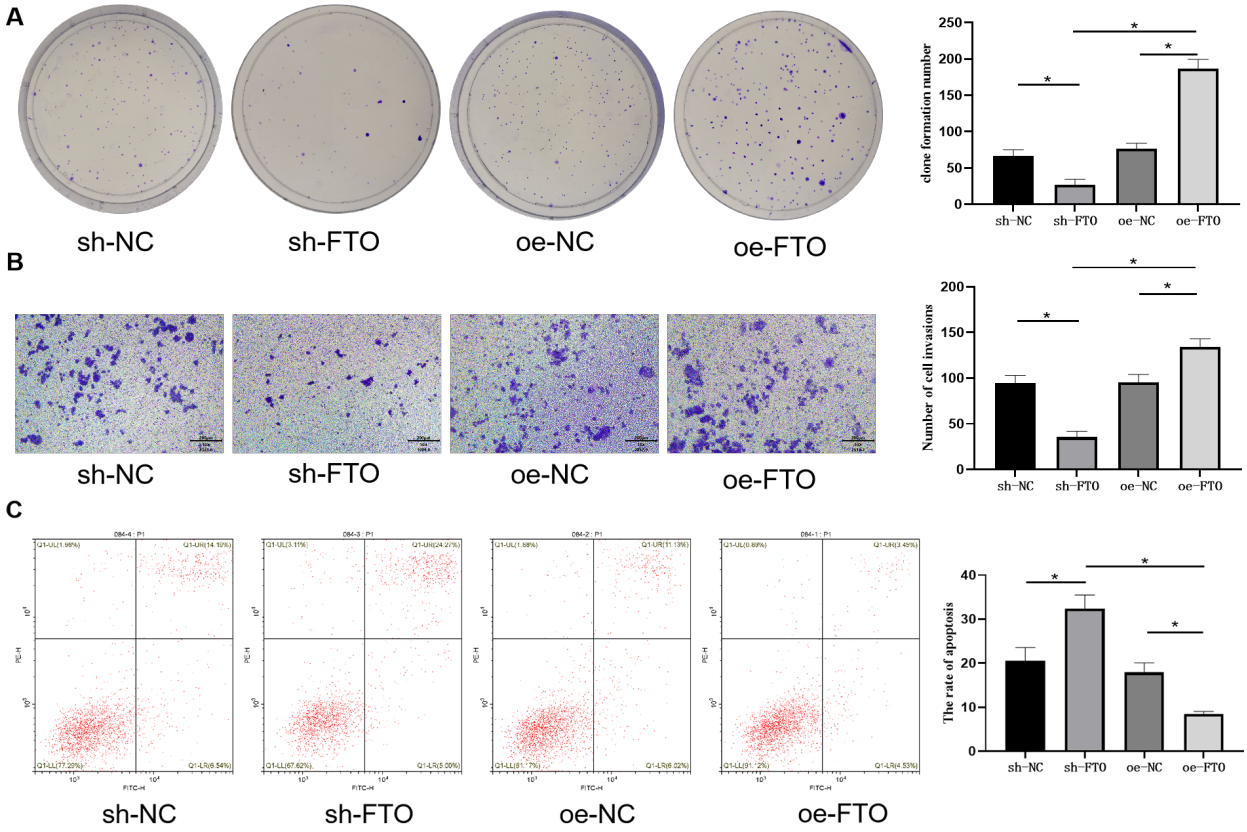

Fig. 3. Overexpression of FTO upregulated HCC cell proliferation and invasion and inhibited apoptosis. (A) Colony formation assay. (B) Transwell assay. (C) Annexin V assay of hepatocellular carcinoma (HCC) cell. Scale = 200 μm. *$p < 0.05$.

animal under certain clinical conditions: when it loses 20 to 25% of its body weight, when it exhibits malignant or wasting symptoms, or when the size of the solid tumor exceeds 10% of the animal's body weight. The experimental design was approved by the Animal Ethics Committee of The Affiliated Nahua Hospital (ethical approval number: 2022-ky-134).

H&E Staining

The tissue samples were fixed with 4% paraformaldehyde followed by decalcification with 10% EDTA for 20 days. After this, they were sliced into 5 μm sections and deparaffinized in xylene for 30 minutes followed by ethanol treatment. Subsequently, the tissue sections were washed sequentially with distilled water and PBS and subjected to H&E staining. Finally, the stained tissue sections were observed using a microscope (ECS005783, Eclipse Ci, Nikon, Shanghai, China).

Statistical Analysis

For statistical significance, each experiment was conducted three times. The data were presented as the mean values with corresponding standard deviations ($\bar{x} \pm s$). Statistical differences among various experimental groups were assessed using one-way ANOVA followed by the Dunnett post hoc test. Statistical significance was considered at a p-value < 0.05. Moreover, the data obtained through histopathological examination were analyzed using Image-Pro Plus 6.0 software (MEDIA CYBERNETICS Image Technology Inc., New York, NY, USA).

Results

Overexpression of FTO Downregulated m^{6}A Methylation of XBP1 in HCC Cell

The FTO was knocked down and overexpressed in HepG2 cells, and the cells were divided into the FTO overexpressed group (oe-FTO), overexpression control group (oe-NC), FTO knocked-down group (sh-FTO), and control of FTO knocked-down group (sh-NC). The correlation between FTO and XBP1 was assessed using the MeRIP-qPCR method, aiming to evaluate the effect of FTO overexpression and silencing on m^{6}A methylation modification levels of XBP1. As shown in Fig. 1A–C, a specific interaction was observed between *FTO* and *XBP1* mRNA in HCC cells, suggesting that XBP1 may be regulated at the RNA level by interacting with FTO. Furthermore, the sh-FTO group exhibited a substantial increase in the m^{6}A methylation level of XBP1 when compared to the sh-NC and oe-NC groups. Conversely, the methylation level was significantly decreased in the oe-FTO group (Fig. 1D, $p < 0.05$).

Journal of
BIOLOGICAL REGULATORS
and Homeostatic Agents

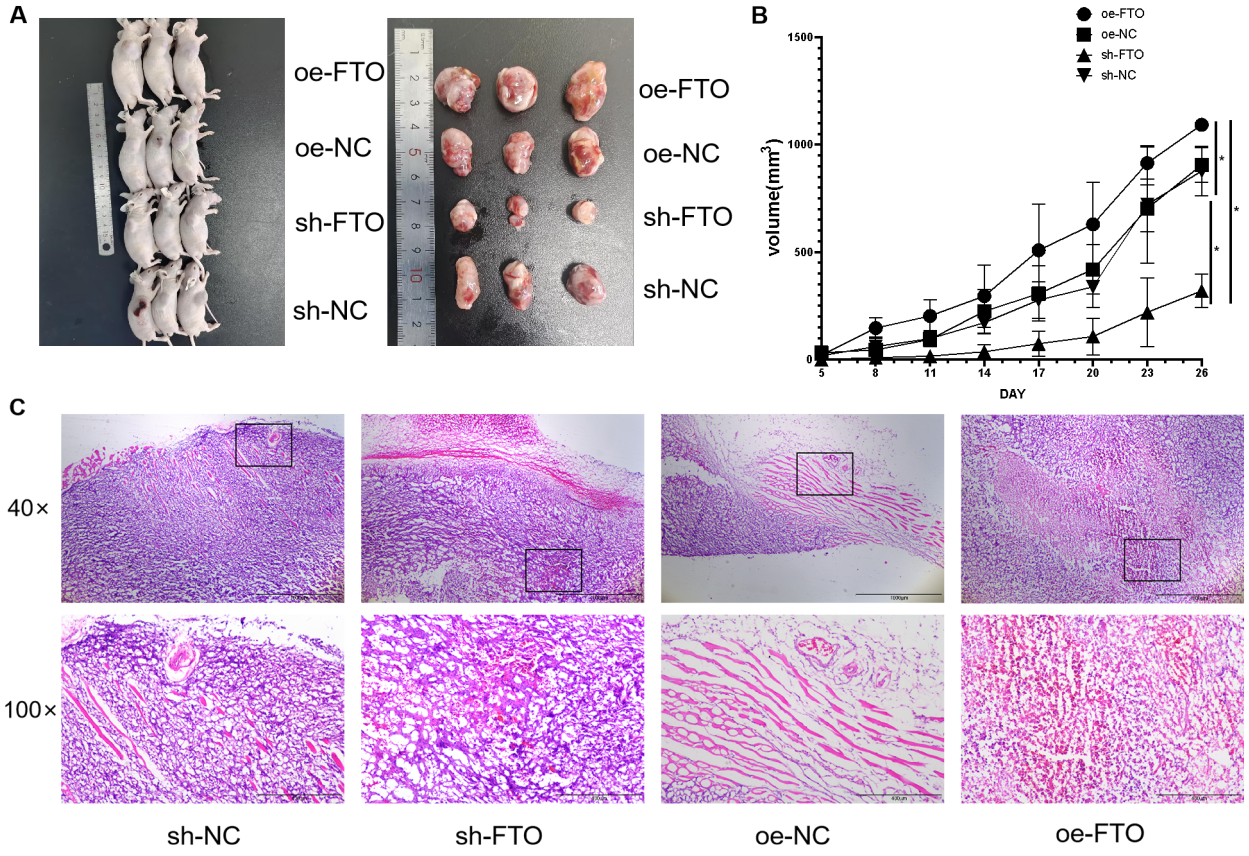

Fig. 4. Over-expression of FTO promoted tumor occurrence and growth in HCC mice. (A) Effects of overexpressed or knocked down FTO on tumor size. (B) Tumor volume change in each group. (C) Hematoxylin-Eosin (H&E) staining was used to observe the effects of overexpressed or knocked-down FTO on tumor occurrence in each group of mice. The scale is 40×, 100×. Scale = 1000 μm, scale = 400 μm. n = 30. *$p < 0.05$.

Overexpression of FTO Upregulated the Expression of XBP1 and C/EBPα in HCC Cells

The expression levels of XBP1 and C/EBPα were determined across all experimental groups using quantitative real time polymerase chain reaction (qRT-PCR) and Western blotting (WB) techniques. As depicted in Fig. 2A,B, when compared to the sh-NC and oe-NC groups, the expressions of FTO, XBP1, and C/EBPα, both at mRNA and protein levels, were significantly reduced in the sh-FTO group ($p < 0.05$). However, they were substantially elevated in the oe-FTO group ($p < 0.05$). Hence, the upregulation of C/EBPα expression in HCC cells was observed in response to the overexpression of FTO.

Overexpression of FTO Upregulated HCC Cell Proliferation and Invasion and Inhibited Apoptosis

HCC cell proliferation, invasion, and apoptosis were assessed through colony formation assay, Transwell assay, and Annexin V assay, respectively. As depicted in Fig. 3A–C, the sh-FTO group exhibited a significant reduction in proliferation and invasion levels compared to the sh-NC and oe-NC groups. However, the apoptosis rate was significantly increased in the sh-FTO group. Conversely, the oe-FTO group displayed the opposite trends, with increased proliferation and invasion levels and decreased apoptosis rate compared to sh-NC and oe-NC groups ($p < 0.05$). These findings suggest that FTO overexpression upregulates proliferation and invasion of HCC cells while inhibiting apoptosis.

Over-Expression of FTO Promoted Tumor Occurrence and Growth in HCC Mice

Cells in each group were digested, centrifuged, washed, and resuspended in PBS. The cell suspension (1×10^6/mL) was injected subcutaneously into BALB/c mice to establish a transplanted tumor model. The animals were divided into the oe-FTO, oe-NC, sh-FTO, and sh-NC groups. After 4 weeks, the mice in each group were euthanized and the tumors were extracted. The tumor size, weight, and occurrence time were observed. As shown in Fig. 4A,B, the tumor in the oe-FTO group showed rapid growth, reaching about 1450 mm^3 by day 26. Conversely, tumor growth in the oe-NC and sh-NC groups was slower than that of oe-FTO, with tumor volume about 950 mm^3 on the 26th day. However, in the sh-FTO group, tumor growth was moderate, with tumor volume about 200 mm^3 by day 26.

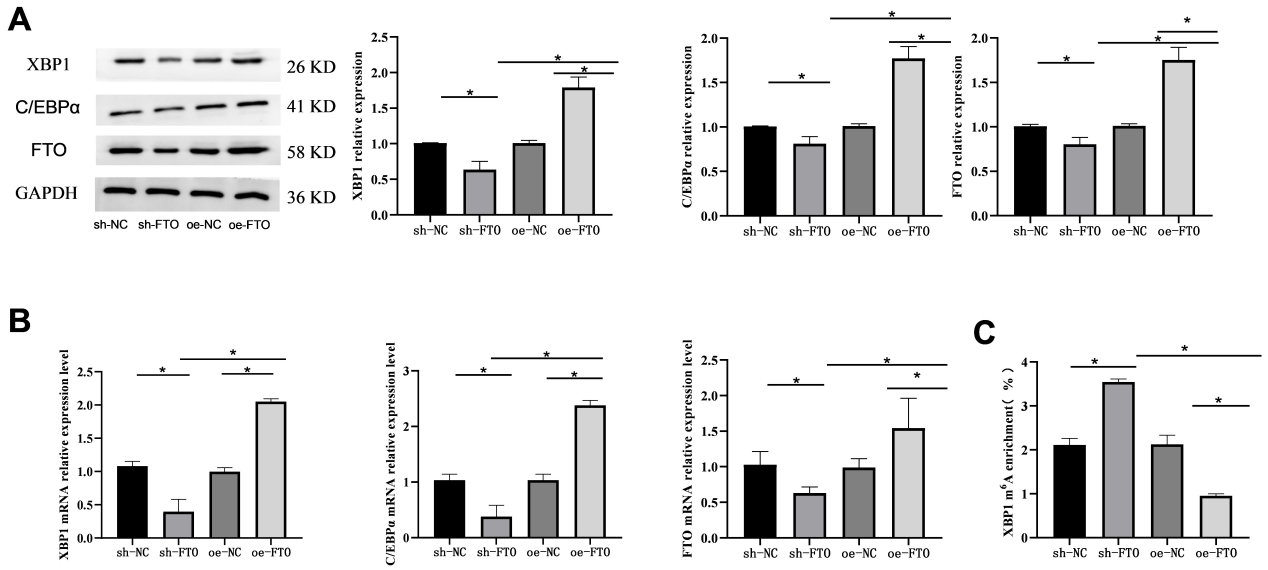

Fig. 5. Overexpression of FTO downregulated m^{6}A methylation level of XBP1 and upregulated the expression of XBP1 and C/EBPα in HCC mice. (A) The expression levels of XBP1, C/EBPα, and FTO proteins were determined using WB analysis. (B) The levels of *XBP1*, *C/EBPα*, and *FTO* mRNA were assessed using PCR. (C) MeRIP-qPCR was used to examine the effects of FTO overexpression and knockdown on XBP1 m^{6}A methylation levels. *$p < 0.05$. n = 30.

Furthermore, pathological changes in tumors from each group were evaluated employing H&E staining. As shown in Fig. 4C, the tumor showed vigorous growth in the oe-FTO group, whereas the tumor growth was inhibited in the oe-NC group. Through microscopic examination, partial growth inhibition with partial injury was observed in the sh-FTO group, along with partial growth inhibition in the sh-NC group.

Overexpression of FTO Downregulated m^{6}A Methylation Level of XBP1 and Upregulated the Expression of XBP1 and C/EBPα in HCC Mice

The mRNA and protein expression levels of XBP1 and C/EBPα in each group of mice were evaluated using qRT-PCR and WB techniques. Additionally, RIP-qPCR was employed to assess the m^{6}A modification level of XBP1 in the tumor tissue of each group. As depicted in Fig. 5A–C, the m^{6}A methylation level of XBP1 was significantly increased in the sh-FTO group, while decreased in the oe-FTO group, in comparison to the sh-NC and oe-NC groups. Furthermore, relative to the sh-NC and oe-NC groups, the sh-FTO group exhibited a significant reduction in the expression of FTO, XBP1, and C/EBPα, both at mRNA and protein levels. Conversely, their expression levels were significantly elevated in the oe-FTO group ($p < 0.05$).

Discussion

Globally, HCC ranks as the fifth most prevalent cancer. Among men, it holds the fourth position in terms of common cancers and is the second leading cause of death. Furthermore, men are highly susceptible to HCC compared to women [15]. The primary contributors to HCC include hepatitis B and C virus infection, alcohol use disorder, and non-alcoholic fatty liver disease [16]. The pathogenesis of HCC is a complex process involving a range of molecular mechanisms, including disruption of the cell cycle, changes in DNA methylation, chromosomal instability, immune system modulation, epithelial-mesenchymal transition, proliferation of HCC stem cells, and miRNA dysregulation. However, the typical progression of disease involves liver injury, chronic inflammation, fibrosis, cirrhosis, and eventually resulting in the development of HCC [17]. Importantly, aberrant DNA methylation emerges as an initial event in the onset of various tumor types [18]. Research indicates that DNA methylation markers in HCC tumor tissues correlate with the survival rate of patients who undergo early surgical tumor resection, providing prognostic value for survival outcomes [19].

m^{6}A is the most abundant internal RNA modification in eukaryotes, and studies have shown that m^{6}A methylation plays a significant role in diverse biological processes, including lipid metabolism [20], hepatocyte inflammation [21], non-alcoholic fatty liver disease [22], liver tumorigenesis, and metastasis. Therefore, targeting specific m^{6}A regulators may provide potential therapeutic interventions for these diseases. FTO, serving as an m^{6}A demethylase, has been reported to play a significant role in promoting acute myeloid leukemia [23] and breast cancer [24]. In the present study, FTO overexpression was found to catalyze XBP1 m^{6}A demethylation, thereby regulating XBP1-C/EBPα to promote the growth of hepatocellular carcinoma.

Journal of
BIOLOGICAL REGULATORS
and Homeostatic Agents

During tumorigenesis and progression, cancer cells frequently encounter endoplasmic reticulum (ER) stress induced by various factors, including glucose deprivation, hypoxia, DNA damage, or calcium deficiency within the ER. The unfolded protein response (UPR), serving as an adaptive mechanism, enables tumor cells to navigate these pathophysiological challenges effectively [25]. Investigating how the UPR influences tumor components, whether by activation or inhibition, and exploring the potential of cancer therapy targeting the UPR, present promising avenues for curbing tumor growth and improving cancer outcomes [26]. XBP1s emerged as a crucial player among the UPR regulators. ER stress induced by reactive oxygen species activates inositol-requiring enzyme 1, initiating cytoplasmic alternative splicing of *XBP1* mRNA. This splicing event leads to a frameshift, ultimately resulting in the production of spliced mRNA encoding the XBP1 spliced form protein [27]. The IRE1/XBP1 pathway holds significance in bolstering tumor survival under ER stress [28]. XBP1 is overexpressed in diverse solid tumors, including breast cancer and HCC, implying its potential as a novel regulator of tumorigenesis and metastasis across different cancer types. Research revealed elevated expression of XBP1s in liver cancer group compared to the control group, closely linked to distant metastasis and poor prognosis in liver cancer. Both *in vitro* and *in vivo* experiments have substantiated that XBP1s promoted the epithelial-mesenchymal transition (EMT) of liver cancer cells through the Twist/Snail pathway [29].

As a member of the CCAAT/enhancer binding protein family, C/EBPα acts as a pivotal transcription factor, playing a significant role in regulating cell differentiation, proliferation, as well as glucose and lipid metabolism. Notably, the function of C/EBPα in tumors appears to be context-dependent. In certain environment, C/EBPα functions as a tumor suppressor by impeding cell proliferation and fostering terminal differentiation. However, it is often silenced or mutated through promoter hypermethylation [30]. However, in HCC, upregulated C/EBPα expression is linked to poor patient survival. This regulatory relationship involves C/EBPβ influencing the expression of XBP1, consequently impacting the expression of C/EBPα, a pivotal adipogenic factor. Moreover, the interaction of XBP1 and IREα can stimulate the C/EBPα promoter, activating its expression during adipogenesis. Whether the regulation of HCC by FTO is involved in ER stress and adipose differentiation and whether the development of NAFL is controlled by FTO remain to be elucidated.

Conclusion

The overexpression of FTO catalyzes m^6A demethylation of XBP1, thereby orchestrating the regulation of both XBP1 and C/EBPα expressions. This process impedes cell apoptosis, consequently fostering the initiation and progression of HCC.

Availability of Data and Materials

Data are available from the corresponding authors upon reasonable request.

Author Contributions

CX and LJJ contributed equally to the conception and design of the research study, acquisition of data, analysis and interpretation of the data, and drafting of the manuscript. XZL provided technical support in the acquisition of data and performed statistical analysis. WL provided expertise in the field of study and contributed to the interpretation of the data. All authors contributed to editorial changes in the manuscript. All authors read and approved the final manuscript. All authors have participated sufficiently in the work and agreed to be accountable for all aspects of the work.

Ethics Approval and Consent to Participate

This study was conducted in accordance with the Guide for the Care and Use of Laboratory Animals adopted and promulgated by the United Nations National Institutes of Health (NIH Publication No.85-23, revised 1996). The experimental design was approved by the Animal Ethics Committee of The Affiliated Nanhua Hospital (ethical approval number: 2022-ky-134).

Acknowledgment

Not applicable.

Funding

This study is supported by Key guidance topic of Hunan Provincial Health Commission (202104010743), Hengyang City Guiding Plan Project ([2021] No.51-120) and Hengyang City Guiding Plan Project (202222035832).

Conflict of Interest

The authors declare no conflict of interest.

References

[1] Ren Z, Ma X, Duan Z, Chen X. Diagnosis, Therapy, and Prognosis for Hepatocellular Carcinoma. Analytical Cellular Pathology. 2020; 2020: 8157406.

[2] Sidali S, Trépo E, Sutter O, Nault JC. New concepts in the treatment of hepatocellular carcinoma. United European Gastroenterology Journal. 2022; 10: 765–774.

[3] Meng Z, Ren Q, Zhong G, Li S, Chen Y, Wu W, *et al*. Noninvasive Detection of Hepatocellular Carcinoma with Circulating Tumor DNA Features and α-Fetoprotein. The Journal of Molecular Diagnostics. 2021; 23: 1174–1184.

[4] Wang Z, Qin H, Liu S, Sheng J, Zhang X. Precision diagnosis of hepatocellular carcinoma. Chinese Medical Journal. 2023; 136: 1155–1165.

[5] Duan JL, Chen W, Xie JJ, Zhang ML, Nie RC, Liang H, *et al*. A novel peptide encoded by N6-methyladenosine modified circMAP3K4 prevents apoptosis in hepatocellular carcinoma. Molecular Cancer. 2022; 21: 93.

[6] Li Y, Qi D, Zhu B, Ye X. Analysis of m6A RNA Methylation-Related Genes in Liver Hepatocellular Carcinoma and Their Correlation with Survival. International Journal of Molecular Sciences. 2021; 22: 1474.

[7] Liu X, Zhang Y, Wang Z, Liu L, Zhang G, Li J, *et al*. PRRC2A Promotes Hepatocellular Carcinoma Progression and Associates with Immune Infiltration. Journal of Hepatocellular Carcinoma. 2021; 8: 1495–1511.

[8] Shen C, Xuan B, Yan T, Ma Y, Xu P, Tian X, *et al*. m^6A-dependent glycolysis enhances colorectal cancer progression. Molecular Cancer. 2020; 19: 72.

[9] Li Q, Ni Y, Zhang L, Jiang R, Xu J, Yang H, *et al*. HIF-1α-induced expression of m6A reader YTHDF1 drives hypoxia-induced autophagy and malignancy of hepatocellular carcinoma by promoting ATG2A and ATG14 translation. Signal Transduction and Targeted Therapy. 2021; 6: 76.

[10] Wang Y, Wang Y, Gu J, Su T, Gu X, Feng Y. The role of RNA m6A methylation in lipid metabolism. Frontiers in Endocrinology. 2022; 13: 866116.

[11] Berulava T, Buchholz E, Elerdashvili V, Pena T, Islam MR, Lbik D, *et al*. Changes in m6A RNA methylation contribute to heart failure progression by modulating translation. European Journal of Heart Failure. 2020; 22: 54–66.

[12] Yin H, Zhang X, Yang P, Zhang X, Peng Y, Li D, *et al*. RNA m6A methylation orchestrates cancer growth and metastasis via macrophage reprogramming. Nature Communications. 2021; 12: 1394.

[13] Zhang W, Xiao P, Tang J, Wang R, Wang X, Wang F, *et al*. m6A Regulator-Mediated Tumour Infiltration and Methylation Modification in Cervical Cancer Microenvironment. Frontiers in Immunology. 2022; 13: 888650.

[14] Tao L, Mu X, Chen H, Jin D, Zhang R, Zhao Y, *et al*. FTO modifies the m6A level of MALAT and promotes bladder cancer progression. Clinical and Translational Medicine. 2021; 11: e310.

[15] Lin Z, Wan AH, Sun L, Liang H, Niu Y, Deng Y, *et al*. N6-methyladenosine demethylase FTO enhances chemo-resistance in colorectal cancer through SIVA1-mediated apoptosis. Molecular Therapy. 2023; 31: 517–534.

[16] Liu Z, Wang M, Wang X, Bu Q, Wang Q, Su W, *et al*. XBP1 deficiency promotes hepatocyte pyroptosis by impairing mitophagy to activate mtDNA-cGAS-STING signaling in macrophages during acute liver injury. Redox Biology. 2022; 52: 102305.

[17] Wang Q, Bu Q, Liu M, Zhang R, Gu J, Li L, *et al*. XBP1-mediated activation of the STING signalling pathway in macrophages contributes to liver fibrosis progression. JHEP Reports: Innovation in Hepatology. 2022; 4: 100555.

[18] Wei M, Nurjanah U, Herkilini A, Huang C, Li Y, Miyagishi M, *et al*. Unspliced XBP1 contributes to cholesterol biosynthesis and tumorigenesis by stabilizing SREBP2 in hepatocellular carcinoma. Cellular and Molecular Life Sciences. 2022; 79: 472.

[19] Tsai HW, Chen YL, Wang CI, Hsieh CC, Lin YH, Chu PM, *et al*. Anterior gradient 2 induces resistance to sorafenib via endoplasmic reticulum stress regulation in hepatocellular carcinoma. Cancer Cell International. 2023; 23: 42.

[20] Hashimoto A, Sarker D, Reebye V, Jarvis S, Sodergren MH, Kossenkov A, *et al*. Upregulation of C/EBPα Inhibits Suppressive Activity of Myeloid Cells and Potentiates Antitumor Response in Mice and Patients with Cancer. Clinical Cancer Research. 2021; 27: 5961–5978.

[21] Zhao Y, Yu Z, Ma R, Zhang Y, Zhao L, Yan Y, *et al*. lncRNA-Xist/miR-101-3p/KLF6/C/EBPα axis promotes TAM polarization to regulate cancer cell proliferation and migration. Molecular Therapy. Nucleic Acids. 2020; 23: 536–551.

[22] Xu Z, Meng SH, Bai JG, Sun C, Zhao LL, Tang RF, *et al*. C/EBPα Regulates FOXC1 to Modulate Tumor Growth by Interacting with PPARγ in Hepatocellular Carcinoma. Current Cancer Drug Targets. 2020; 20: 59–66.

[23] Xie G, Wu XN, Ling Y, Rui Y, Wu D, Zhou J, *et al*. A novel inhibitor of N^6-methyladenosine demethylase FTO induces mRNA methylation and shows anti-cancer activities. Acta Pharmaceutica Sinica. B. 2022; 12: 853–866.

[24] Chidambaranathan-Reghupaty S, Fisher PB, Sarkar D. Hepatocellular carcinoma (HCC): Epidemiology, etiology and molecular classification. Advances in Cancer Research. 2021; 149: 1–61.

[25] Villanueva A. Hepatocellular Carcinoma. The New England Journal of Medicine. 2019; 380: 1450–1462.

[26] Ogunwobi OO, Harricharran T, Huaman J, Galuza A, Odumuwagun O, Tan Y, *et al*. Mechanisms of hepatocellular carcinoma progression. World Journal of Gastroenterology. 2019; 25: 2279–2293.

[27] Jung G, Hernández-Illán E, Moreira L, Balaguer F, Goel A. Epigenetics of colorectal cancer: biomarker and therapeutic potential. Nature Reviews. Gastroenterology & Hepatology. 2020; 17: 111–130.

[28] Villanueva A, Portela A, Sayols S, Battiston C, Hoshida Y, Méndez-González J, *et al*. DNA methylation-based prognosis and epidrivers in hepatocellular carcinoma. Hepatology. 2015; 61: 1945–1956.

[29] Yang Z, Yu GL, Zhu X, Peng TH, Lv YC. Critical roles of FTO-mediated mRNA m6A demethylation in regulating adipogenesis and lipid metabolism: Implications in lipid metabolic disorders. Genes & Diseases. 2021; 9: 51–61.

[30] Barajas JM, Lin CH, Sun HL, Alencastro F, Zhu AC, Aljuhani M, *et al*. METTL3 Regulates Liver Homeostasis, Hepatocyte Ploidy, and Circadian Rhythm-Controlled Gene Expression in Mice. The American Journal of Pathology. 2022; 192: 56–71.